

Reply to anonymous Referee #1 (acpd-14-C11680–C11684)

This study compares trajectories in the TTL calculated with three different temperature datasets. The focus of the evaluation is on the statistical evaluation of the minimum temperature along the trajectories as they cross the tropical tropopause, and the corresponding water vapour entering the stratosphere. It is shown that the overall humidity values and in particular the seasonal cycle and interannual variability are only very weakly sensitive to the choice of the temperature dataset. The objective of the study is well justified and the results are in principle relevant; however, important aspects of the paper are not well explained and/or conceptually fuzzy - as outlined in my comments below. Therefore major revisions are required to turn this study into a fully consistent and convincing paper.

Reply:

Thanks for those helpful comments. We have made substantial changes to the manuscript to include answers to all aspects. The detailed answers for each question can be found below, with line numbers from the updated manuscript.

Major comments:

A) Is this paper really about the impact of "temperature resolution"? First, the study only considers the vertical resolution aspect, and not the horizontal nor the temporal one. In particular temporal resolution might also matter, but this is not mentioned in the paper. Then, "resolution" to me sounds very technical (e.g., like running a model with two different resolutions). But this is not exactly the problem, nor what you do. My point is that if the MERRA assimilation cycle was running with a model with higher vertical resolution, then the resulting field would not necessarily capture more of the, e.g., gravity wave signals because capturing them is not only an issue of resolution but also of the representation of the wave triggering mechanisms. I would like the authors to discuss more critically and explicitly what they actually do. I think it is good and relevant, but it is not well described by "resolution". Maybe then the authors might also consider rephrasing the title of their study.

Reply:

This is an excellent point. We intend to investigate the impacts of vertical variability of tropopause temperatures on trajectory modeling of water vapor. It is known that local tropopause temperature could experience much variability in the vertical, so the real question is that if the temperature datasets we used already captured enough variability in tropopause temperature. If not, how big impact could it be? In the updated manuscript, we have changed the title to "... temperature vertical variability..." to make the objective of this paper clearer.

B) Three datasets are used and I am perfectly fine with the first two of them: MERRA is used because it is "standard", available for a long time period etc. GPS is used

because it is based upon independent observations with fine vertical resolution. My expectation is that this data set should be as close to reality as possible. But then why use the synthetically created MERRA-Twave dataset? I understand that this dataset would be valuable if we did not have GPS. But since we have GPS what can this dataset tell us in addition? I suggest to better motivate the use of this third dataset, or to focus on the analysis with MERRA and GPS only.

Reply:

We included both GPS and MER-Twave datasets because they have their own advantages and limitations. GPS provides sparse sampling in the tropics (only ~800-1100 profiles per day), which means the variability in GPS is smaller than reality, although its mean is more accurate given the precise profiling. In contrast, MER-Twave has better variability but not accurate mean, since it is designed to have similar temperature variability to radiosondes but with mean reserved to original MERRA data (Kim and Alexander, 2013). In summary, the mean temperature is closer to reality in GPS than in MER-T and MER-Twave, but the temperature variability is closer to reality in MER-Twave than in MER-T and GPS. We have added this discussion in lines 240-249.

- C) *The discussion of the impact of atmospheric waves is insufficient. The general statement at the beginning of section 2.2.2 "Waves are underrepresented in reanalyses" does not make sense. Clearly planetary and synoptic-scale waves are/should be perfectly captured by reanalyses. It remains unclear, which part of the wave spectrum is considered here. Kelvin waves, gravity waves? When discussing the role of, e.g., gravity waves on the temperature field in the TTL, then maybe also the temporal resolution should be discussed. Six-hourly fields, from MERRA or GPS, cannot capture the temporal propagation / evolution of waves. This could potentially also affect the minimum temperature along the trajectories.*

Reply:

The description of underrepresented waves can be found in Kim and Alexander, 2013. According to their results (their Fig. 1b-d), at reanalysis model levels temperature variability at time scales shorter than ~10 days are weaker than observations. Thus, underrepresented waves include a part of Kelvin waves, mixed Rossby-gravity waves, and gravity waves. However, the problem in using reanalysis data for trajectory simulations is associated not only with these waves (< 10 days), but also with slow-scale waves (>10 days), since it involves interpolation between reanalysis vertical levels. As shown in Kim and Alexander, 2013, conventional interpolation (either linear or higher order) in-between model vertical levels degrades temperature variability even at longer time scales (> 10 days). This is because observed temperature profiles have strong curvatures in-between coarse model levels due to the existence of fine vertical-scale waves.

We only considered a vertical resolution issue, since horizontal or temporal resolution of current reanalyses is good enough to resolve most of TTL waves (Note that we do not mean that horizontal and temporal resolutions are good enough to resolve wave generation mechanisms.). A large portion of TTL waves has horizontal

and temporal scales much larger and longer than reanalysis resolution, therefore, temperature behaves almost linearly in-between model horizontal and temporal resolution. However, temperature does not behave linearly in vertical space due to the fact that a significant portion of TTL waves have vertical wavelengths shorter than ~4 km (see Figure S4 in supporting information of Kim and Alexander, 2015), which could make waves less represented by the ~1.2 km vertical resolution in reanalyses.

The above discussion has been included in section 2.2.2.

D) *The paper has not been very carefully written. Several sentences/formulations are unclear:*

- *p. 29210 line 11: what is meant by "finite resolution"? Every resolution is finite, do you mean "fine"? (This problem occurs in several places.)*

Reply:

Yes, we mean fine resolution. All “finite” have been corrected to “fine”.

- *p. 29213 line 15: "the carrying methane" sounds odd to me. Not clear how the methane values are initialized in the trajectories.*

Reply:

Corrected. We have modified in lines 122-126 to include the whole story of methane carried in our model.

- *p. 29213 line 19: what is meant by "limited in the tropical 110-50 hPa"?*

Reply:

Tropical 110-50 hPa is where the most dehydration happens. Refer Fig. 5a-c.

- *p. 29213 line 28: "total diabatic heating rates from all sky": please explain this better.*

Reply:

It means total heating rates due to long-wave and short-wave radiation, moist physics, friction, etc. It has been modified in lines 95-97.

- *p. 29214 line 8: "not represented well in current coarse model levels": you probably mean "... in models with coarse vertical resolution"; but I think this is not really the point (see comment A): even with more levels MERRA would not correctly capture all gravity waves emitted from tropical convection.*

Reply:

Agree. See reply to question C and more detailed explanation in section 2.2.2.

- *p. 29217 line 5: what is "the curly nature" of a temperature profile?*

Reply:

The “curly nature” means the strong curvature of temperature profiles around the cold-point tropopause. This has been rephrased in line 253-255.

- p. 29220 line 4: "We see slightly drier air in GPS run expected"?

Reply:

Rephrased.

- p. 29220 line 20: The sentence "Note that ..." is too long, and it is not clear what is meant by "the two are strongly coupled".

Reply:

Rephrased. See lines 367-369.

- E) p. 29215 lines 24: This is an interesting result, but it is not well discussed. How can these happen? How can MERRA be too cold at model levels (compared to GPS) but too warm in between? MERRA values in between model levels are calculated by linear interpolation and therefore I would expect that a cold bias at the model levels is "transferred" to the layer in between.

Reply:

MERRA doesn't assimilate GPS observations, which makes these two datasets independent from each other. Within the tropopause MERRA model levels are separated ~ 1.2 km apart, which might miss the temperature variations that could only be captured by data in finer vertical resolutions, such as GPS observations. Therefore, although MERRA is warmer at model levels, it doesn't necessarily mean MERRA should be warmer in-between. This is clearly shown in Fig. R11a-b below.

Moreover, the mean temperature differences depend on the location being examined. For example, if we only consider the deep inner tropics (10° N-S), MERRA shows warm biases throughout the entire tropopause layers (Fig. R11c). Either way, a clear fact is that MERRA is warm biased at the cold-point tropopause (~ 100 -90 hPa).

This discussion has been added in the discussions of Fig. 2.

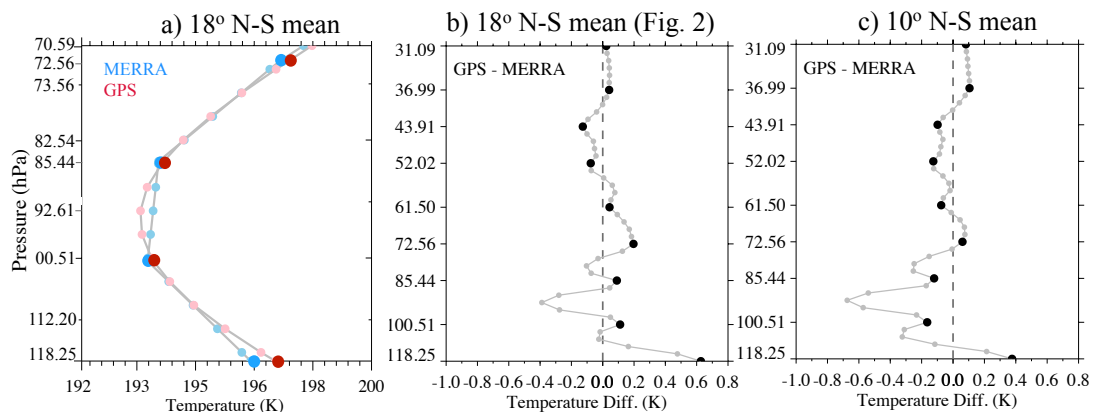


Figure R11. a) MERRA and GPS temperature averaged within 18° N-S in 2007-2013; b) the differences in a); and c) same as b) but averaged within 10° N-S. Clearly average within different latitudes results in different values, but the warm bias in MERRA cold-point tropopause always exists.

F) *In section 3.1 I have a problem in understanding the selection of the trajectories. My impression is that trajectories are selected if they reach the 90-hPa level (this is considered as the entry point in the stratosphere). This is fine with me, but this implies that (during the time period considered) some trajectories maybe don't reach the 60- hPa level. But then you determine FDP statistics up to 60 hPa! Does this not lead to a biased distribution? Should you not select trajectories that reach 60 hPa instead of 90 hPa?*

Reply:

Our trajectory model runs forward, and along time we kept records of any dehydration occurrences. Starting from the initiation level 370-K, parcels ascend to higher altitudes while crossing the tropopause, during which parcels experience multiple dehydrations whenever colder temperatures were encountered. On the other hand, parcel's water vapor is conserved when encountering warmer temperature. To isolate the FDP events, we chose parcels that were already above 90-hPa for at least six months since the last time they were dehydrated (FDP). This guarantees that parcels already crossed the cold-point tropopause (~ 380 K or ~ 100 -94 hPa) and experienced their final dehydration. This part has been modified accordingly in section 3.1, lines 276-283.

G) *p. 29218 line 19: The bimodal FDP distribution with MERRA data is interesting (Fig. 5). But in principle the distribution should be even more peaked! When using linear interpolation between model levels, then minimum temperature must occur exactly at one of the model levels. So the smearing out of the two peaks is an effect of the temporal resolution of the trajectory output. I assume that you determine the minimum temperature from 6-hourly values along the trajectories. Then of course it can happen that the time when the trajectory reaches the exact pressure of a model level is "hidden" (i.e., in between two times) and therefore the "real" location and value of the minimum temperature is missed. This indicates that the temporal resolution can play an important role, and I suggest that the role of temporal resolution (of the wind fields, of the trajectory output) is discussed in the paper.*

Reply:

This is an excellent point. Along the trajectory integration, FDP is where the coldest temperature is encountered along a parcel's path. This coldest temperature could be found either exactly at MERRA model levels or in-between levels during that step of integration, depending on the trajectory integration intervals. As shown in Fig. R12 below: during two steps of integration (from $t \rightarrow t+\Delta t$, and from $t+\Delta t \rightarrow t+2\Delta t$), the FDP could be found exactly at (Fig. R12a), above (Fig. R12b), or below (Fig. R12c) the MERRA cold-point level (85.4 hPa). Suppose our trajectory integration interval is as small as seconds then at some time steps parcels would inevitably travel to each of the MERRA model levels, and therefore the encountered coldest temperatures would always be at either of the two model levels in MERRA. In another word, the bimodal FDP distribution from MERRA run could be even more peaked when choosing smaller integration step. Two reasons that we didn't choose

such small time step: 1) the wind and temperature data are only available 6-hourly or even daily (GPS), so much smaller time step introduces more uncertainties with more interpolation; 2) considering the balance between model running speed and computational resources. This has been addressed in context lines 312-322.

Currently we output trajectory results on daily basis, which is already fine enough to study the evolutions of FDP on monthly or seasonal basis. Besides, due to the domain-filling feature of our model, the FDP results are not sensitive to longer, such as 3-day or 5-day, or shorter, such as hourly, output intervals.

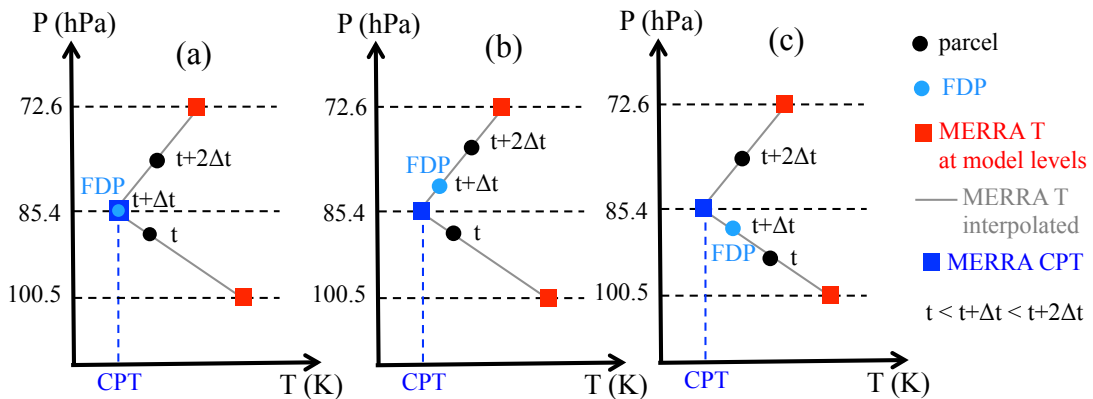


Figure R12. Illustration of the FDP locations in different scenario. Filled squares are MERRA temperatures at model levels, with cold-point tropopause (CPT) marked in blue and others in red. Grey lines are linearly interpolated temperatures in-between model levels. Parcels (black dots) travel from t , to $t+\Delta t$, and then to $t+2\Delta t$. During this process, FDP (blue dots) could be found exactly at MERRA model levels (a) or in-between MERRA model levels (b, c).

Minor comments:

1) *p. 29212 line 8: maybe a terminology detail: here you write about "resolved but underrepresented waves" - does this (see comment A) also indicate that your study is not mainly about resolution, but more about "effects of gravity(?) waves on the temperature field"?*

Reply:

We realized that “resolution” is not appropriate in expressing our objective, so we changed it to “vertical variability”. The MER-Twave has more variability than standard MERRA temperatures.

2) *Section 2.2.2 is very difficult to understand. If you keep this MERRA-Twave dataset in your study, this paragraph should become less technical (for the technical aspects the reader can be referred to Kim and Alexander 2013). Here the reader should be able to learn the general concept.*

Reply:

Agree. Now we have shortened the technical explanations and replaced with more discussions of waves and temperature variability in section 2.2.2.

- 3) *Comparing Figs. 5 and 7b: something is probably not correct with the scales of the FDP events. Values in Fig. 7b are about 4 times smaller, but in both cases they should integrate to 100%.*

Reply:

For both Fig. 5 and Fig. 7b, the FDP occurrence frequencies are calculated as the ratio of FDP events at each 2-hPa bin relative to total FDP events, regardless of seasons, within the 110-60 hPa range. Therefore, the curves in Fig. 5 represent the mean FDP frequencies averages in all seasons, and the integration of each curve is 100% before being normalized to “%/hPa” (i.e., frequencies divided by 2-hPa). Fig. 7b, however, only shows the frequencies of FDP during SON relative to all season FDP, therefore its magnitude is about ¼ of total frequencies.

In the updated manuscript, we have changed all normalized FDP frequency unit in Fig. 5 from “%/hPa” to “%”, so each PDF profile integrate from bottom to up ends up with 100%.

Editorial comments:

- p. 29213 line 19: *"Noted" should read "Note"*

Reply:

Corrected.

- p. 29214 line 9: *should read "... that use an idealized parameterization of..."*

Reply:

Corrected.

[Reference]

Kim, J.-E., and Alexander, J. M.: A new wave scheme for trajectory simulations of stratospheric water vapor, *Geophys. Res. Lett.*, 40, 5286–5290, doi:10.1002/grl.50963, 2013.

Kim, J.-E., and Alexander, J. M.: Direct impacts of waves on tropical cold point tropopause temperature, *Geophys. Res. Lett.*, doi:10.1002/2014GL062737, 2015.

Reply to anonymous Referee #2 (acpd-14-C9976–C9981)

This study discusses an important scientific question, namely inter annual variability of stratospheric water vapour. The particular focus is on trajectory calculations and on the question in how far the vertical resolution of the information on stratospheric temperatures influences the simulated freeze drying in the model. This is an interesting and important topic, which is of interest to the readership of ACP.

The descriptions of a trend in water vapour and interannual and seasonal variability are different things (e.g. Ploeger et al., 2011; Fueglistaler et al., 2013) and are likely influenced by different processes. And the issue of stratospheric water vapour trends is an important issue, which is alluded to in the manuscript, but somewhat underrepresented in the discussions here. Note that stratospheric trends of water vapour are rather uncertain (e.g., Hurst et al., 2011; Kunz et al., 2013; Urban et al., 2014; Hegglin et al., 2014). It would be important, if this paper could provide further and deeper insight into the interpretation of stratospheric water vapour trends. Alternatively, if the focus of the paper is solely on variability, this should be clearly stated in the paper.

Reply:

Like we said, the focus of our paper is to investigate the impacts of temperature datasets on the trajectory modeling of water vapor, so we have removed all discussion of “trend” in this version. It is not appropriate to analyze decadal trend based on only ~7 years of data. Besides those papers that discussed H₂O trend based on Boulder records (Hurst et al., 2011; Kunz et al., 2013), which were later proved to be problematic (Hegglin et al., 2014), we have a new paper published recently (Dessler et al., 2014) on the uncertainties of H₂O trend.

A major focus of the paper is on dehydration mechanisms of stratospheric air and Figure 5 is the central figure. However I have reservations about the figure and its interpretation (see also below). From the concept of FDP presented in this figure, it is not clear to me why the stratospheric water vapour levels can be so similar for the three temperature sources given the fact that the FDP curves are rather similar, but the FDP frequencies are rather different. I think the paper could be clearer here in its arguments.

Reply:

The different shapes of FDP curves are caused by whether the tropopause temperatures have enough variability in the vertical. In case of MERRA, the tropopause temperatures are constrained only at two discrete levels (100 and 85 hPa), and therefore the FDP peaks around them. In case of GPS and MER-Twave, enough variability in tropopause temperatures enables FDP to be found in a wider range, and therefore the FDP curves going through gradual transitions.

The dashed curves of FDP H₂O represent the stratosphere entry level of H₂O, controlled solely by the coldest temperatures that parcels encountered along their travelling paths. When FDP occurs at tropopause level (90-100 hPa), the entry level H₂O could have generally 0.1-0.4 ppmv differences comparing between MERRA and GPS

(Fig. 4 and Fig. 8), which is not easy to tell given the large upper x-axis range in Fig. 5. That's why the dashed curves look similar, but still different. In the updated Fig. 5, we have plotted FDP and FDP H₂O in four seasons as well as all season averages.

I also suggest that an actual reconstruction of a water vapour profile is presented in the paper not only FDP profiles or relative water vapour differences (Fig. 8). This should allow a better assessment of the quality of the simulated profiles.

Reply:

We have updated this figure as Fig. 7 in the updated manuscript to include the actual water vapour profiles from three different runs.

Further, I suggest the authors consider the effect of methane oxidation on the increase of water vapour with altitude. Note that the chemical conversion of methane to water vapour (which does not occur through photolysis, see below) does not have to happen at altitudes of 80 or 60 hPa. Rather aged air that has experienced methane oxidation will descend and could be mixed into these altitudes (Ploeger et al., 2012; Abalos et al., 2013). In the presented model study, this effect is likely only partly taken into account by just considering trajectories. Could this be relevant for the results of this paper? The effect should be easy to check in a model world by switching off methane oxidation in the model. I suggest that the authors conduct such a sensitivity test and compare with observed water vapour profiles.

Reply:

Aged air descending back to the tropics has very limited impacts on the dehydration and final water vapour abundances in the lower stratosphere. This has been shown in our previous paper (refer Fig. 6 in Schoeberl et al., 2012). A more quantitative impression can be understood in Fig. R21 below, where trajectory results are obtained from using GPS temperatures with methane oxidation turned on and off. It is clear that below 70 hPa (~19 km), aged parcels carrying H₂O from methane oxidation plays a trivial role in the overall abundances of water vapour. This has been addressed in the updated manuscript in lines 126-128.

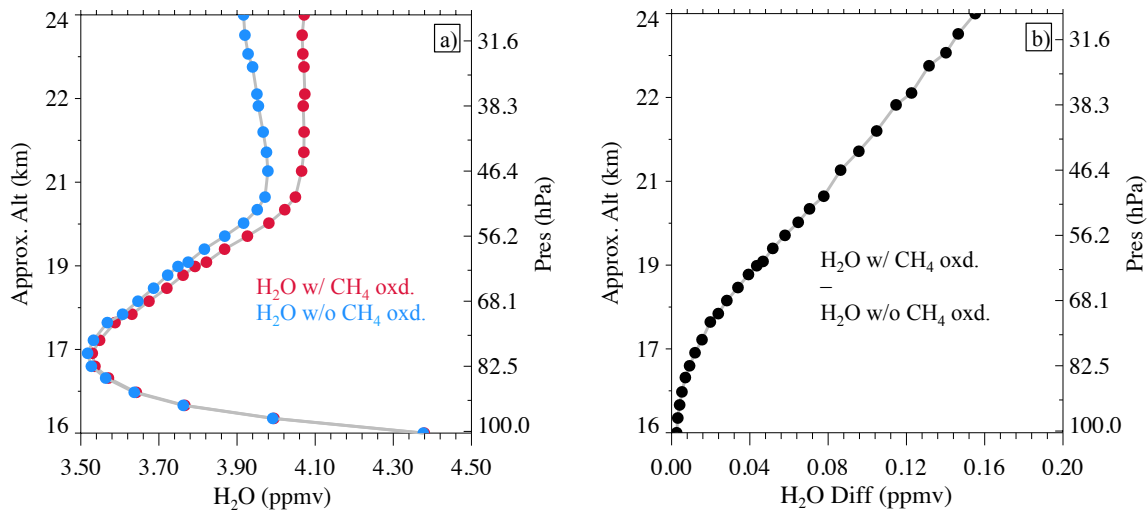


Figure R21. (a) Trajectory simulated water vapour from using GPS temperatures, with methane oxidation turned on (red) and off (blue); (b) The differences caused by methane oxidation. All data are averaged over the tropics (18° N-S) in 2007-2013.

The paper also makes the point that inter annual variability is unchanged in the time series when the different temperature sets are employed and ‘only’ the absolute value is affected. First it should be discussed and stated in the paper that the absolute values are important for calculating the radiative forcing (and thus for the climate impact). In my opinion, the absolute values matter. Second, what is the conclusion from this observation? That high and low excursions in the interannual variability are equally affected by the resolution of the temperatures? Should this conclusion also hold for time series longer than the seven years shown in Fig. 9? For example, for time series over 30 years with pronounced variability?

Reply:

This is an excellent point. We have added discussions of the importance of H_2O abundances to the radiative forcing calculations.

One of the conclusions of this paper is that despite the different vertical resolutions of temperature, the predicted water vapour interannual variability is almost the same. This conclusion also holds for longer time period as shown in Fig. R22 below. This discussion has been added in section 3.2.

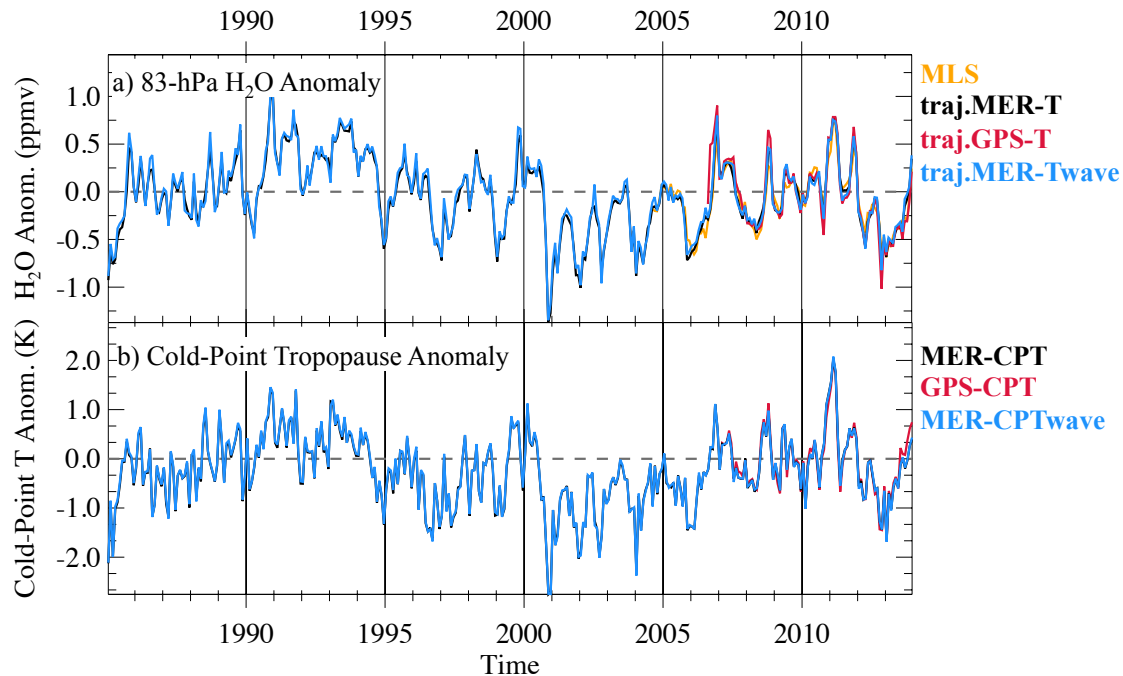


Figure R22. The H₂O anomaly (a) and the cold-point tropopause anomaly in longer period from different datasets.

Comments in detail

- *p. 29211., l. 4: Is immediate freeze out at 100% saturation assumed? This statement seems to imply that this is the case. How realistic is this assumption? For example Tompkins et al. (2007) argued for a different representation of dehydration in the ECMWF model and other trajectory studies have tested different dehydration assumptions.*

Reply:

We performed sensitivity tests to different saturation levels and it turns out that the simulated water vapour offset constant values but with identical interannual variability. Note that the major focus of this paper is to investigate the uncertainty introduced by using temperatures in different vertical resolutions. Despite the frequent occurrences of supersaturation (Jensen et al., 2013) and the re-evaporation of the condensate (e.g., Schoeberl et al., 2014), the comparison would be essentially the same as long as we keep the same criteria for different runs. This discussion is included in the update manuscript lines 116-120.

- *p. 29212., l. 20: It should be more explicitly stated which terms enter the calculation of the potential temperature tendency here; just clear sky heating rates?*

Reply:

We used total diabatic heating rates from all sky, which include heating rates from long-wave and short-wave radiation, moist physics, friction, etc. This has been modified in lines 75-97 to be clear.

- *p. 29213., l. 18: The major chemical loss of methane in the stratosphere occurs through reactions with radicals, not through photolysis (e.g. Röckmann et al., 2004; Brasseur and Solomon, 2005); if the loss mechanism used here is really photolysis, the loss (and thus the water vapour production) is not correctly simulated.*

Reply:

Oxidation of hydrogen, mainly methane, is an important in situ source of water vapour in the stratosphere. To account for methane oxidation in our model, we independently track methane in each parcel and photolyze it using photochemical loss rates. The loss of each molecule of methane produces two molecules of H₂O (Dessler et al., 1994). The oxidation of H₂ formed from methane photolysis is implicitly included in this scheme. This has been stated in the updated manuscript lines 122-128.

Minor issues

- *Abstract, l. 11: 1.2 km is also finite, do you mean 'higher resolution'*
- *Abstract, l. 11: 'including' is incorrect, you only consider there tow data sets.*
- *p. 29211., l. 15: 'tracers that depend'*
- *p. 29211., l. 23: 'carrying H2O' is unclear*
- *p. 29212., l. 1: drop 'etc.'*
- *p. 29213., l. 2: why 're' entered?*
- *p. 29214., l. 9: 'that used' . . .*

Reply:

Done the above.

- *p. 2921., l. 27: state how the 0.4 ppmv bias was deduced*

Reply:

We have added temperature profiles in Fig. 2. Averaged over 18° N-S, the largest temperature difference of 0.4 K shows at ~93 hPa (cold-point tropopause) when the GPS temperature is generally ~193 K. With 100% saturation level assumption, the C-C equation yields a 0.41 ppmv difference in H₂O. This has been added in the updated manuscript lines 193-197.

- *p. 29216: l. 19: how do we know it is 'realistic'?*

Reply:

The MER-Twave is designed to have similar temperature variability to radiosondes measurements based on Kim and Alexander, 2013. Temperature variability in radiosondes measurements can be treated as realistic.

- *Figure 5: The text states that the analysis was done using a large number of isentropic trajectories, nonetheless, Fig. 5 looks as if the analysis has been done on several discrete pressure levels. See for example the obvious kinks in the black solid line, which are spaced about 5 hPa apart. Further, it looks to me that the solid lines in Fig 7b and in Fig 5 are the same lines, although the x-axis is different. Please check.*

Reply:

We perform diabatic trajectories in isentropic coordinate to avoid the over dispersion in pressure coordinate. After that, we present results in pressure coordinate to be able to compare with reanalyses model levels, which are pressure levels.

Fig. 5 is the FDP frequency averaged over 7 years, whereas Fig. 7b only shows the SON season. The reason that x-axis is different is because the frequencies are calculated with respect to the total FDP events in 7 years, therefore the magnitude in Fig. 7b is about $\frac{1}{4}$ of that in Fig. 5. This has been modified in the updated Fig. 5 to relative to the FDP events of each curve.

In the updated Fig. 5, we have changed all normalized FDP frequency unit from “%/hPa” to “%”, so each PDF profile integrate from bottom to up ends up with 100%.

- *p. 29221., l. 2: change ‘stratospheric’ to ‘stratosphere’*

Reply:

Done.

[References]

- Dessler, A. E., Schoeberl, M. R., Wang, T., Davis, S. M., Rosenlof, K. H., and Vernier, J.-P.: Variations of stratospheric water vapor over the past three decades, *J. Geophys. Res. Atmos.*, 119, 12,588–12,598, doi:10.1002/2014JD021712, 2014.
- Dessler, A.E., Weinstock, E. M., Hints, J. G., Anderson, J. G., Webster, C. R., May, R. D., Elkins, J. W., and Dutton, G. S., An examination of the total hydrogen budget of the lower stratosphere. *Geophysical Research Letters*, 21: 2563–2566. doi: 10.1029/94GL02283, 1994.
- Hegglin, M. I., Plummer, D. A., Shepherd, T. G., Scinocca, J. F., Anderson, J., Froidevaux, L., Funke, B., Hurst, D., Rozanov, A., Urban, J., von Clarmann, T., Walker, K. A., Wang, H. J., Tegtmeier, S., and Weigel, K.: Vertical structure of stratospheric water vapour trends derived from merged satellite data, *Nature Geoscience*, 7, 768–776, doi:10.1038/ngeo2236, 2014.
- Hurst, D. F., Oltmans, S. J., Vömel, H., Rosenlof, K. H., Davis, S. M., Ray, E. A., Hall, E. G., and Jordan, A. F.: Stratospheric water vapor trends over Boulder, Colorado: Analysis of the 30 year Boulder record, *J. Geophys. Res.*, 116, D02306, doi:10.1029/2010JD015065, 2011.
- Jensen, E. J., Diskin, G., Lawson, R. P., Lance, S., Bui, T. P., Hlavka, D., McGill, M., Pfister, L., Toon, O. B., and Gao, R.: Ice nucleation and dehydration in the Tropical Tropopause Layer, *Proc. Natl. Acad. Sci.*, 110, 2041–2046, 2013.
- Kim, J.-E., and Alexander, J. M.: A new wave scheme for trajectory simulations of stratospheric water vapor, *Geophys. Res. Lett.*, 40, 5286–5290, doi:10.1002/grl.50963, 2013.
- Kunz, A., Müller, R., Homonnai, V., Jánosi, I., Hurst, D., Rap, A., Forster, P., Rohrer, F., Spelten, N., and Riese, M.: Extending water vapor trend observations over Boulder into the tropopause region: trend uncertainties and resulting radiative forcing, *J. Geophys. Res.*, 118,

11 269–11 284, doi:10.1002/jgrd.50831, 2013.
Schoeberl, M. R., Dessler, A. E., Wang, T., Avery, M. A, Jensen, E.: Cloud Formation,
Convection, and Stratospheric Dehydration, Earth and Space Science, DOI:
10.1002/2014EA000014, 2014.

1 **The impact of temperature resolution vertical variability**
2 **on trajectory modeling of stratospheric water vapour**

3

4 **T. Wang^{1,2}, A. E. Dessler¹, M. R. Schoeberl³, W. J. Randel⁴, J.-E. Kim⁵**

5 [1]{Texas A&M University, College Station, Texas}

6 [2]{NASA Jet Propulsion Laboratory/California Institute of Technology, Pasadena, California}

7 [3]{Science and Technology Corporation, Columbia, Maryland}

8 [4]{National Center for Atmospheric Research, Boulder, Colorado}

9 [5]{University of Colorado, Boulder, Colorado}

10 Correspondence to: Tao Wang (Tao.Wang@jpl.nasa.gov)

11

12 **Abstract**

13 Lagrangian trajectories driven by reanalysis meteorological fields are frequently used to
14 study water vapour (H₂O) in the stratosphere, in which the tropical cold-point
15 temperatures regulate H₂O amount entering the stratosphere. Therefore, the accuracy of
16 temperatures in the tropical tropopause layer (TTL) is of great importance for
17 **understanding stratospheric H₂O abundances trajectory—studies**. Currently, most
18 reanalyses, such as the NASA MERRA (Modern Era Retrospective-Analysis for
19 Research and Applications), only provide temperatures with ~1.2 km vertical resolution
20 in the TTL, which has been argued **misses realistic variability in tropopause temperatures**
21 **and therefore** introduce uncertainties in **our understanding of stratospheric H₂O**. In this
22 paper, we quantify this uncertainty by comparing the **Lagrangian** trajectory models using
23 MERRA temperatures on **standard** model levels (*traj.MER-T*), to those using

24 temperatures with more vertical variability at the tropopause. This includes GPS
25 temperatures (*traj.GPS-T*) in finer vertical resolution and adjusted MERRA temperatures
26 with enhanced variability induced by underrepresented waves ~~but underrepresented by~~
27 ~~the current model levels~~ (*traj.MER-Twave*). It turns out that enhanced vertical variability
28 in tropopause temperature more realistically simulates captures the dehydration of air
29 entering the stratosphere. ~~pattern in, therefore the bimodal dehydration peaks in~~
30 ~~*traj.MER-T* due to limited vertical resolution disappear in *traj.GPS-T* and *traj.MER-*~~
31 ~~*Twave*, by allowing the cold-point tropopause to be found at finer vertical levels.~~
32 ~~Comparing with *traj.MER-T*, *traj.GPS-T* has little impact on simulated stratospheric H₂O~~
33 ~~(changes~~ But the effect on H₂O abundances is relatively minor: comparing with
34 *traj.MER-T*, *traj.GPS-T* tends to dry air by ~0.1 ppmv while *traj.MER-Twave* tends to dry
35 air by 0.2-0.3 ppmv. Despite these differences in absolute values of predicted H₂O and
36 vertical dehydration patterns, there is virtually no difference in the interannual variability
37 in different runs. Overall, we find that tropopause temperature ~~in~~ with finer vertical
38 resolution variability has limited impact on predicted stratospheric H₂O ~~in the trajectory~~
39 ~~model.~~

40

41 1. Introduction

42 Stratospheric water vapour (H₂O) and its feedback play an important role in regulating
43 the global radiation budget and the climate system (e.g., Holton et al., 1995; Randel et al.,
44 2006; Solomon et al., 2010; Dessler et al., 2013). It has been known since Brewer's
45 seminal work on stratospheric circulation that tropical tropopause temperature is the main
46 driver of stratospheric H₂O concentration (Brewer, 1949). As parcels approach and pass
47 through the cold-point tropopause – the altitude at which air temperature is coldest,

48 condensation occurs **and ice falls out**, thereby **regulating** the parcel's H₂O concentration
49 to local saturation level (e.g., Fueglistaler et al., 2009, and references therein). This is the
50 dehydration process. The role of tropopause temperature variation in **tropical** dehydration
51 is most apparent in the annual variation in tropical stratospheric H₂O, also known as the
52 “tape recorder” (Mote et al., 1996).

53

54 When air crosses **enters** the tropical tropopause layer (TTL), it experiences multiple
55 dehydrations due to encounter of **colder** lower temperatures, and the final stratospheric
56 H₂O mixing ratio is established after air passing through the coldest temperature **along its**
57 **path**, which sets the strong relation between cold-point tropopause and the entry level
58 H₂O (e.g., Holton and Gettelman, 2001; Randel et al., 2004, 2006).

59

60 The details of the transport and dehydration process can be understood by performing
61 Lagrangian trajectory simulations, which track the temperature history of a large number
62 of individual parcels. Unlike **simulating** simulation of chemical tracers that depends
63 strongly on the transport imposed (Ploeger et al., 2011; Wang et al., 2014), the simulation
64 of H₂O is primarily constrained by tropopause temperatures. Dehydration thus primarily
65 depends on the air parcel temperature history, and stratospheric H₂O simulations
66 ultimately require accurate analyses of temperatures particularly in the tropopause (e.g.,
67 Mote et al., 1996; Fueglistaler et al., 2005, 2009; Liu et al., 2010; Schoeberl and Dessler,
68 2011; Schoeberl et al., 2012, 2013).

69

70 In this paper, we use a forward, domain-filling trajectory model to study the detailed

71 dehydration behavior of the humidity of air parcels ~~and the carrying H₂O in entering~~ the
72 tropical lower stratosphere. Previous analyses have demonstrated that this model can
73 accurately simulate many of the aspects of the observed stratospheric H₂O (Schoeberl and
74 Dessler, 2011; Schoeberl et al., 2012, 2013). Despite the good agreements with
75 observations, there are clear areas of uncertainty, such as the accuracy of circulation
76 fields (Schoeberl et al., 2012), the details of the dehydration mechanisms (Schoeberl et
77 al., 2014), the influences from convection (Schoeberl et al., 2011, 2014), and the impacts
78 of unresolved temperature variability in the TTL, etc. In this paper, we investigate
79 uncertainties introduced by the last one – the effect of vertical resolution variability of
80 temperatures.

81

82 ~~We will examine the impacts of reanalysis temperature in relatively coarse vertical~~
83 ~~resolutions on trajectory simulations of stratospheric H₂O.~~ This is accomplished by
84 comparing trajectory results from using NASA Modern Era Retrospective-Analysis for
85 Research and Applications (MERRA) (Rienecker et al., 2011) temperatures at standard
86 model levels, to using temperatures with finer vertical variability, which include GPS
87 temperatures and the MERRA temperatures adjusted to account for resolved but
88 underrepresented waves (Kim and Alexander, 2013) ~~to using GPS temperatures and the~~
89 ~~MERRA temperatures adjusted to account for resolved but underrepresented waves (Kim~~
90 ~~and Alexander, 2013), both in finer vertical resolution.~~ This will help us to further
91 understand the importance of tropopause temperature variability in dehydrating
92 dehydration of air entering the stratosphere.

93

94 **2. Trajectory Model and Temperatures Used**

95 **2.1 Trajectory model**

96 The trajectory model used here follows the details described in Schoeberl and Dessler
97 (2011) with ~~trajectories—calculated~~ parcel positions integrated using the Bowman
98 trajectory code (Bowman, 1993; Bowman et al., 2013). This model has been proven ~~to be~~
99 ~~able to simulate~~ capable of simulating stratosphere H₂O and its long-term variability
100 (Schoeberl and Dessler, 2011; Schoeberl et al., 2012, 2013; Dessler et al, 2014), modeling
101 chemical tracers transport in the lower stratosphere (Wang et al., 2014), and studying the
102 stratosphere air age spectrum (Ray et al., 2014). Because of the overly dispersive
103 behavior of kinematic trajectories (e.g., Schoeberl et al., 2003; Liu et al., 2010; Ploeger et
104 al., 2010; Schoeberl and Dessler, 2011), we perform diabatic trajectories using isentropic
105 coordinates, in which the vertical velocity is the potential temperature tendency converted
106 from the diabatic heating rates via the thermodynamic equation (e.g., Andrews et al.,
107 1987). Here we used total heating rates, which include heating due to long-wave and
108 short-wave radiation, moist physics, friction, etc.

109

110 The parcel initiation level is chosen to be the 370-K isentrope, which is above the level of
111 zero radiative heating (~355-365 K, Gettelman and Forster, 2002) and below the tropical
112 tropopause (~375–380 K) in the tropics. Every day, parcels are initialized on equal area
113 grids covering 40°N–40°S and advected forward in time by reanalysis winds. At the end
114 of each day, any parcels that have descended below the 345 K (~250 hPa or ~10 km)
115 level are removed since in most cases they have ~~re-~~entered the troposphere. The upper
116 boundary is chosen to be 2200 K isentrope (~1 hPa or ~50 km) to cover the entire

117 stratosphere. Parcels are initialized and added to the ensemble consecutively on every day
118 and the combined set of parcels is then advected forward. This process is repeated over
119 the entire integration period so that after 2-3 years the stratospheric domain is filled up
120 with parcels – this is the concept of domain-filling, ~~that~~ which guarantees a robust
121 statistics.

122

123 H₂O is conserved along the trajectories, except when saturation occurs; in that case, ~~then~~
124 excess ~~of~~ H₂O is instantaneously removed from the parcel to keep the relative humidity
125 with respect to ice from exceeding 100%. This is sometimes referred as “instant
126 dehydration” (e.g., Schoeberl et al., 2014), ~~which This simple scheme that~~ ignores
127 detailed microphysics ~~but has shown to and has been proven to be able to~~ simulate many
128 features of H₂O in the lower stratosphere (e.g., Fueglistaler et al., 2005; Jensen and
129 Pfister, 2004; Gettelman et al., 2002). ~~We chose the 100% saturation level because 1)~~
130 ~~different saturation levels offset the simulated H₂O constant values but with identical~~
131 ~~interannual variability; and 2) the focus of the paper is to investigate the uncertainty~~
132 ~~introduced by using different temperatures, which would be the same as long as we keep~~
133 ~~the same criteria for different runs.~~

134

135 In addition to H₂O, we also carry methane (CH₄) concentration for each parcel. We
136 initiate CH₄ values increased from 1.76 ppmv in 2006 to 1.83 ppmv in 2013. ~~For each~~
137 ~~parcel, we also consider H₂O oxidized from the carrying methane.~~ As described in
138 Schoeberl and Dessler (2011), we use photochemical loss rates supplied from Goddard
139 two-dimensional stratospheric chemistry model (Fleming et al., 2007) to ~~photolyze~~

140 convert each methane molecule into two molecules of H₂O (Dessler et al., 1994). Noted
141 that our analysis focus on the tropical lower stratosphere, ~~all results in this paper are~~
142 ~~limited in the tropical 110-50 hPa~~, where methane oxidation has little impacts on the total
143 H₂O abundances (Fig. 6 in Schoeberl et al., 2012).

144

145 Along each trajectory, we locate the point when air experiences coldest temperature as
146 the final dehydration point (FDP), which determines the stratosphere entry level H₂O
147 mixing ratio (FDP-H₂O) for that trajectory. As will be shown below, the entry level H₂O
148 predicted by the trajectory model is affected by the vertical variability in temperature
149 field.

150

151 **2.2 Temperature datasets**

152 In this paper, we use MERRA (Rienecker et al., 2011) circulation to advect parcels. This
153 includes horizontal wind components and total diabatic heating rates. As shown in
154 Schoeberl et al. (2012, 2013), trajectory model driven by this reanalysis yields excellent
155 estimates of H₂O compared to observations by the Aura Microwave Limb Sounder
156 (MLS) (Read et al., 2007).

157

158 Driven by the same circulation, we use three different temperature datasets to quantify
159 the uncertainty induced by temperatures with different variability in the vertical: 1)
160 MERRA standard temperatures on model levels (MER-T), denoted as *traj.MER-T*; 2)
161 GPS radio occultation (RO) temperatures, denoted as *traj.GPS-T*; and 3) MERRA
162 temperatures enhanced by wave scheme to recover the variability not represented well in

163 current coarse model levels (Kim and Alexander, 2013), denoted as *traj.MER-Twave*.
164 ~~Different from earlier papers that uses an idealized parameterizations of waves added to~~
165 ~~the temperature datasets (e.g., Schoeberl and Dessler, 2011), here we amplify waves that~~
166 ~~are underrepresented in the coarse vertical resolution of MERRA temperatures.~~ Note that
167 MERRA does not assimilate GPS observations, which makes the two temperature
168 datasets independent from each other. Trajectory runs with the three different temperature
169 datasets are summarized in Table 1.

170

171 **2.2.1 GPS temperature**

172 Owing to its high vertical resolution, GPS temperature profiles capture the cold-point
173 tropopause ~~with high in-unprecedented~~ accuracy. In this paper we use GPS wet profile
174 (wetPrf) retrieved at 100-m vertical resolution ~~using from~~ a one-dimensional variational
175 technique based on ECMWF analysis. The wetPrf and GPS Atmospheric Profile (atmPrf,
176 derived assuming no water vapor in the air) temperatures are essentially the same in 200-
177 10 hPa but below 200 hPa the errors in atmPrf could be as high as ~ 3 K due to neglect of
178 water vapour (Das and Pan, 2014). Despite being retrieved at 100-m resolution, the actual
179 vertical resolution ranges from 0.5 km in the lower troposphere to ~ 1 km in the middle
180 atmosphere (Kursinski et al., 1997).

181

182 The GPS radio occultation (RO) technique makes the data accuracy independent of
183 platforms. ~~It has been reported that~~ That makes the biases among different RO payloads
184 could be as low as 0.2 K in the UTLS (Ho et al., 2009). Therefore, to compensate the
185 relatively lower horizontal resolution (relative to that of reanalysis), we include GPS RO

186 from all platforms. This includes the Constellation Observing System for Meteorology,
187 Ionosphere, and Climate (COSMIC) (Anthes et al., 2008), the CHALLENGING Minisatellite
188 Payload (CHAMP) satellite (Wickert et al., 2001), the Communications/Navigation
189 Outage Forecasting System (CNOFS), the Gravity Recovery And Climate Experiment
190 (GRACE) twin satellites (Beyerle et al., 2005), the Meteorological Operational Polar
191 Satellite–A (MetOp-A), the Satellite de Aplicaciones Cientifico-C (SACC) satellite (Hajj
192 et al., 2004), and the TerraSAR-X (TerraSAR-X). There are ~2000-3500 profiles per day,
193 mostly from COSMIC, with ~800-1100 profiles of these in the tropics.

194

195 Each day, GPS temperature profiles are binned to 200-m vertical resolution. Horizontally,
196 we grid data into 2.5x1.25 (longitude by latitude) grids with 2-D Gaussian function
197 weighting. This gridded dataset has been successfully used in diagnosing many detailed
198 features of tropopause inversion layer (Gettelman and Wang, 2015). We use over 7 years
199 of GPS data available from July 2006 to December 2013, and the trajectory run using it is
200 denoted as *traj.GPS-T*.

201

202 Fig. 1 shows a snapshot of the 100-hPa GPS raw (panel a) and gridded (panel b)
203 temperature on January 1st, 2010, compared with MERRA temperature (panel c). It
204 demonstrates that the gridded GPS temperature ~~clearly~~ captures most of the variability,
205 although some detailed structure might be lost due to its relatively sparse sampling.

206

207 Fig. 2 shows the GPS and MERRA temperatures ~~in the TTL (panel a) and their~~
208 differences (GPS–MERRA) ~~(panel b, extended to 31 hPa)~~ averaged over the deep tropics

209 (18°S–18°N) during the GPS period. Here, we examine the values at the MERRA model
210 levels (larger dots) as well as MERRA in-between levels (smaller dots), where both GPS
211 and MERRA temperatures are linearly interpolated to the same pressure levels. ~~Here we~~
212 ~~use linear instead of higher order, such as cubic, interpolation because linear scheme~~
213 ~~performs better (see Sect. 2.2.3). As we can see, due to the strong curvature in~~
214 ~~temperature profile,~~ It shows that the GPS is at most ~0.4 K colder than MERRA around
215 the cold-point tropopause (~93 hPa on average, in-between MERRA coarse levels),
216 where temperature is ~193 K. This translates to at most a 0.4 ppmv wet bias in the entry
217 level of stratospheric H₂O, assuming 100% saturation level. Note that the GPS
218 temperatures at MERRA levels 100 and 85 hPa could be lower than that in MERRA if we
219 average over 10°S–10°N, but it does not change the fact that MERRA is always warm
220 biased around the cold-point tropopause. ~~Apparently, within the TTL GPS temperatures~~
221 ~~are warmer at MERRA model levels, but in-between the MERRA levels GPS~~
222 ~~temperatures are colder (as much as ~0.4 K) around the cold-point tropopause (generally~~
223 ~~between 100 and 85 hPa), which would bring at most 0.4 ppmv dry bias in the entry level~~
224 ~~of stratospheric H₂O assuming 100% saturation.~~

225

226 **2.2.2 MERRA temperature adjusted by waves**

227 ~~Waves are underrepresented in reanalyses, therefore a further interpolation in the vertical~~
228 ~~significantly dampens even resolved waves due to relatively coarse vertical resolution (as~~
229 ~~seen in comparisons with high resolution radiosondes; Kim and Alexander, 2013). To~~
230 ~~overcome these limitations, a new wave scheme was developed by Kim and Alexander~~
231 ~~(2013) to recover the underrepresented variability, based on amplitude phase~~

232 ~~interpolation and amplification of waves in reanalysis datasets.~~
233
234 ~~For each month's MERRA temperature profiles, we construct a 90-day time series at each~~
235 ~~level centered on that month. Then the Fourier transformation is applied on the time~~
236 ~~series to obtain amplitudes and phases in frequency domain. Those amplitude and phase~~
237 ~~profiles in real space are then interpolated separately into finer 200-m vertical levels to~~
238 ~~bring back the variability induced by waves. After reconstructing new complex functions~~
239 ~~from the interpolated amplitudes and phases, amplification factors for the four seasons~~
240 ~~are applied to enhance wave variability since waves are already weaker at reanalysis~~
241 ~~levels. The amplification factors are defined as the fractional differences between the~~
242 ~~square roots of power spectra in reanalysis and radiosonde data. Finally, the inverse~~
243 ~~Fourier transformation is applied to bring the time series back to the time domain.~~
244 ~~Applying this scheme on MERRA temperature records yields a new MERRA temperature~~
245 ~~dataset that has realistic variability induced by waves (Kim and Alexander, 2013) and the~~
246 ~~trajectory model performed on this temperature is denoted as **traj.MER-Twave**.~~
247
248 Wave-induced disturbances on tropopause temperatures are underrepresented by current
249 reanalyses (Kim and Alexander, 2013). At the reanalysis model levels, temperature
250 variability at time scales shorter than ~ 10 days are weaker than radiosondes observations
251 (refer Fig. 1b-d in Kim and Alexander, 2013). Those underrepresented waves include a
252 part of the spectrum of Kelvin waves, mixed Rossby-gravity waves, and gravity waves.
253 Moreover, when used in trajectory simulations, conventional interpolation of model level
254 temperatures to in-between levels, either linear or higher order, degrades temperature

255 variability even at longer time scales (> 10 days). This is because observed temperature
256 profiles have strong curvatures in-between coarse model levels due to the existence of
257 fine vertical-scale waves.

258

259 To overcome these limitations, a scheme developed by Kim and Alexander, based on
260 amplitude-phase interpolation and wave amplification from radiosonde observations, has
261 been proven to be effective in recovering the underrepresented variability in reanalysis
262 temperatures (refer Kim and Alexander, 2013 for more details). Applying this scheme on
263 MERRA temperature records yields a new MERRA temperature dataset (MER-Twave)
264 that has more realistic temperature variability induced by waves (refer Fig. 3 in Kim and
265 Alexander, 2013). The trajectory simulation using this temperature dataset is denoted as
266 *traj.MER-Twave*.

267

268 Note that we only considered the vertical resolution issue, since it is by far a limiting
269 factor in representing waves in the TTL. A large portion of a TTL wave spectrum has
270 horizontal and temporal scales much larger and longer than reanalysis resolution,
271 therefore, temperature behaves almost linearly in-between model horizontal and temporal
272 resolution. However, temperature does not behave linearly in vertical space due to the
273 fact that a significant portion of TTL waves have vertical wavelengths shorter than ~ 4 km
274 (see Figure S4 in supporting information of Kim and Alexander, 2015), which could
275 make waves less represented by the ~ 1.2 km vertical resolution in reanalyses.

276

277 The wave scheme produces both positive and negative perturbations to the MERRA

278 temperature profiles, depending on the phase of waves. Overall, the change in
279 temperature induced by waves is less than 2 K (Fig. 3), although in rare cases it can reach
280 5-7 K. Importantly, however, about 80% of the changes in cold-point temperature are
281 negative, with the wave scheme lowering the average cold-point temperatures by ~0.35
282 K. It is this reduction in cold-point temperature that is responsible for the reduction in
283 H₂O entering the stratosphere.

284

285 Note that we included both GPS and MER-Twave datasets because they have their own
286 advantages and limitations. GPS provides sparse sampling in the tropics (only ~800-1100
287 profiles per day), indicating a smaller horizontal variability in GPS than likely exists, but
288 the mean temperatures are more accurate. In contrast, MER-Twave has better variability
289 but not accurate mean, since it is designed to have similar temperature variability to
290 radiosondes but with mean reserved to original MER-T. In summary, the mean
291 temperature is closer to reality in GPS than in MER-T and MER-Twave, but the
292 temperature variability is closer to reality in MER-Twave than in MER-T and GPS. In
293 addition, the MER-Twave is a general technique that could be applied to situations where
294 GPS temperatures are not available (e.g., reanalyses before 2006, climate models).

295

296 **2.2.3 Interpolation scheme**

297 In our studies, we use linear interpolation to estimate the temperature between the fixed
298 levels of temperature data sets. However, some previous analyses have used higher order
299 interpolations, such as cubic spline (e.g., Liu et al., 2010), to make assumptions about the
300 strong curvature of temperature profiles around the cold-point tropopause. In order to

301 determine ~~which approach if linear or cubic spline interpolation~~ is superior, we sample
302 GPS tropical temperature profiles at MERRA vertical levels and then use the two
303 interpolation schemes to reconstruct the full GPS resolution. Then we compare the
304 minimum saturation mixing ratio from the recovered profiles to the minimum calculated
305 from the full resolution GPS profiles.

306

307 Fig. 4a shows the probability distribution of the differences between the minimum
308 saturation mixing ratio in the full-resolution GPS profile and in the two interpolation
309 schemes. On average, the linear interpolation performs better (RMS difference is 0.18
310 and 0.25 ppmv for the linear and cubic spline, respectively). Fig. 4b shows the
311 corresponding probability distribution of the difference of the pressure of this minimum,
312 and the linear interpolation does better for this metric, too (RMS difference is 5.2 and 7.2
313 hPa for the linear and the cubic spline interpolation, respectively). We have also tested
314 higher order spline interpolations and find that none produce lower RMS errors than
315 linear interpolation. Overall, cubic spline interpolation tends to underestimate cold-point
316 temperature (~~sometimes unrealistically to as low as -150 K~~), making the implied H₂O too
317 dry, as noted by Liu et al., (2010). Thus, in our studies we adopted linear interpolation
318 scheme for three different trajectory integrations.

319

320 **3. Trajectory Results**

321 **3.1 Dehydration patterns**

322 The gridded GPS temperatures are available since July 2006, so for fair comparison we
323 start all trajectory runs at that time and run them forward till the end of 2013. For each
324 model run, we calculate statistics of the final dehydration points (FDP) for all parcels

325 entering the stratosphere. We define “parcels entering the stratosphere” as parcels that
326 underwent final dehydration between 45°N–45°S (thus ignoring polar dehydration) and
327 that were **already** at altitudes higher (pressure lower) than 90 hPa **for at least** six months
328 **since the last time they were dehydrated (FDP) after their FDP event**. This **guarantees**
329 **that parcels already crossed the cold-point tropopause (~380 K or ~100-94 hPa) and has**
330 **indeed experienced the coldest temperature along its ascending paths**. Averaging over 7
331 years minimizes the effects of interannual variability.

332

333 **Fig. 5a-c compares the FDP frequency (solid lines) and the FDP H₂O (dashed lines) in**
334 **different seasons among three runs. As mentioned, the FDP H₂O can be understood as the**
335 **stratosphere entry level of H₂O**. In all cases, it is clear that dehydration occurs almost
336 exclusively between 60 and 110 hPa. The ~~dashed lines represent the~~ average FDP H₂O,
337 **which** reaches a minimum at 85 hPa for all runs, meaning parcels dehydrated in its
338 vicinity carry the smallest amount of H₂O into the stratosphere. The relatively high FDP-
339 H₂O above 80 hPa (just above the entry level) comes from the parcels that avoided the
340 tropical cold trap and experienced final dehydration at higher, warmer levels of the
341 stratosphere. Out of ~1.3 millions of parcels in the stratosphere there are only ~0.3%
342 bypassed the cold-point tropopause, and these parcels have little impact on the
343 stratosphere **water vapour**.

344

345 The FDP frequency, however, shows large differences among three runs. The run using
346 MERRA temperature (*traj.MER-T*) yields **an annual** bimodal FDP maxima distinctly at
347 98 and 84 hPa (**Fig. 5a solid black lines**), close to the MERRA model levels 100.5 and

348 85.4 hPa, respectively. The bimodal feature comes from averages between single,
349 prominent peaks during DJF (December-January-February, Fig. 5a, blue) and JJA (June-
350 July-August, Fig. 5a, red), when cold-point tropopause is close to a particular level (DJF
351 to 85 hPa and JJA to 100 hPa) in MERRA (Fig. 5d-e black bars), as well as averages
352 between bi-modal peaks during MAM (March-April-May, Fig. 5a, green) and SON
353 (September-October-November, Fig. 5a, yellow), when tropopause temperature in real
354 atmosphere fall in between the two MERRA levels (Fig. 5f red bars). ~~This occurs because~~
355 ~~the cold-point tropopause is constrained to be near these two levels due to limited vertical~~
356 ~~resolution in MERRA temperature, whereas in real atmosphere it may fall in between~~
357 ~~(see Fig. 7 below).~~ The dehydration profiles implied from using the other two datasets,
358 however, experience smoothed changes due to gradual variations of cold-point altitudes
359 in each season (red and blue bars in Fig. 5d-f). It is clear that more realistic dehydrations
360 (Fig. 5b-c) occur with more variability in tropopause temperature (Fig. 5d-f red and blue
361 bars).

362

363 Note that at FDP, the coldest temperature encountered could be either at MERRA model
364 levels or in-between levels during that step of integration, depending on the trajectory
365 integration intervals. Suppose our trajectory integration time step is as small as seconds,
366 then at some time steps parcels would inevitably travel to each of the MERRA model
367 levels, and therefore the encountered coldest temperatures would always be at either of
368 the two levels in MERRA. In another word, the bimodal FDP distribution from MERRA
369 run (Fig. 5a) could be even more peaked when choosing smaller integration step. Two
370 reasons that we didn't choose such small time step: 1) the wind and temperature data are

371 only available 6-hourly or even daily (GPS) so much smaller time step introduces more
372 uncertainties with more interpolation; and 2) considering the balance between model
373 running speed and computational resources.

374

375 Fig. 6 depicts the vertical distributions of normalized FDP in time (panel a-c) and
376 longitude (panel d-f) sectors for the three different runs. We see that the MERRA coarse
377 model levels do not capture the variations of cold-point tropopause well during MAM
378 and SON, resulting in discontinuous transition of FDP from DJF to MAM, and from JJA
379 to SON (panel a). When using GPS temperatures (panel b) and MERRA temperatures
380 adjusted to recover wave-induced variability (panel c), the dehydration patterns show
381 continuous variations throughout the year. The bimodal feature is more emphasized in the
382 longitudinal-vertical view (panel d), where we can also see that throughout a year the
383 most frequent dehydrations occur over the western tropical pacific region. ~~Take the SON~~
384 ~~for example, the longitudinal distribution of dehydration patterns emphasizes the bi-~~
385 ~~modal feature of using MERRA temperature (panel d), contradictory to contradicting the~~
386 ~~single mode feature of using GPS temperature (panel e) or MERRA temperature adjusted~~
387 ~~by waves (panel f), with enhancements centered at 85 and 98 hPa corresponding to the~~
388 ~~altitudes of most frequent cold point tropopause during DJF and JJA, respectively.~~

389

390 ~~The FDP seasonal changes follow exactly the variations of the cold point tropopause~~
391 ~~represented differently by the three temperature records. During SON, for example, Fig. 7~~
392 ~~shows that the cold point tropopause in GPS temperatures (panel a, red) or MERRA~~
393 ~~temperature adjusted by waves (panel a, blue) can be found most frequently within 100-~~

394 ~~85 hPa in this season. Trajectory runs therefore yield peak FDP occurring at the same~~
395 ~~level (panel b red and blue lines). However, due to lacking of levels between 100 and 85~~
396 ~~hPa in MERRA temperatures, the cold-point tropopause is pushed to one of the two~~
397 ~~closest levels (panel a black bars), resulting in bimodal FDP distributions (panel b black~~
398 ~~line) and is therefore responsible for the discontinuity in FDP shown in Fig. 6a and 6d.~~
399 ~~The same argument applies to the MAM results, too. During DJF and JJA, however, the~~
400 ~~cold-point tropopause is close to a particular level (DJF to 85 hPa and JJA to 100 hPa, not~~
401 ~~shown here), generating a single, prominent dehydration peak.~~

402

403 **3.2 Water Vapour (H₂O)**

404 It is obvious that trajectory simulations using GPS temperatures (*traj.GPS-T*) and
405 MERRA temperatures adjusted by waves (*traj.MER-Twave*) tend to yield more
406 reasonable FDP patterns around the cold-point tropopause (Fig. 5 solid lines), although
407 the parcels dehydrated at particular altitudes have similar amounts of H₂O in all three
408 models (FDP H₂O, Fig. 5 dashed lines). A more interesting question is whether the
409 different dehydration occurrences affect the stratospheric H₂O predicted by the trajectory
410 model.

411

412 Fig. 7a shows ~~compare~~ the tropical (18°N–18°S) H₂O profile predicted from three
413 trajectory runs compared with MLS observations. The vertical bars in MLS indicate the
414 MLS vertical resolutions at each of the MLS retrieval pressure levels. Here, we see
415 clearly that the H₂O in stratosphere reflects the different cold-point temperatures in three
416 datasets. The differences induced more variability in temperatures are clearly shown in
417 Fig. 7b, where we see slightly drier air expected in GPS run since GPS temperatures are

418 at most ~ 0.4 K lower than that of MERRA around the tropopause (Fig. 2); whereas
419 enhanced wave perturbations produce air 0.2-0.3 ppmv drier, in agreement with previous
420 calculations (e.g., Jensen et al., 2004; Schoeberl et al., 2011).

421

422 Fig. 8c also shows that comparing to *traj.MER-T*, the dry biases from using GPS
423 temperatures are largest in MAM and SON (0.14-0.21 ppmv on average), when the real
424 cold-point tropopause cannot be resolved by the MERRA model levels. During DJF and
425 JJA, when the cold point is near one of the two MERRA standard levels, the differences
426 become smaller. Thus we conclude that using GPS temperatures decreases simulated
427 stratospheric H₂O by an average of ~ 0.1 ppmv, accounting for $\sim 2.5\%$ given typical
428 stratospheric H₂O abundances of ~ 4 ppmv.

429

430 It is important to point out that, despite these differences in the absolute value of H₂O,
431 there is virtually no difference in the anomalies (~~remainder from the average annual cycle~~
432 ~~remainder after the annual cycle has been subtracted~~). In Fig. 8a we compare the time
433 series of H₂O anomalies at 83 hPa from ~~the~~ three different trajectory runs weighted by the
434 MLS averaging kernels as well the MLS observations. Note that the interannual
435 variations of approximately ± 0.5 ppmv in H₂O are in good agreement with the ~~year-to-~~
436 ~~year~~ interannual changes of about ± 1 K in cold-point tropopause temperatures (Fig. 8b)
437 for all three different runs, further supporting ~~the knowledge~~ that ~~the stratospheric entry~~
438 ~~level of H₂O and cold-point tropopause temperature~~ ~~the two~~ are strongly coupled (e.g.,
439 Randel et al., 2004, 2006; Randel and Jensen, 2013). We also compared *traj.MER-T* and
440 *traj.MER-Twave* over longer period (1985-2013) and it shows almost no differences in

441 interannual variability, either. Clearly, for studying the interannual variability of H₂O,
442 MERRA temperatures in coarse vertical resolution are as good as temperatures in higher
443 vertical resolution.

444

445 **4. Summary**

446 ~~The domain-filling, forward trajectory model is a useful tool in examining the regulation~~
447 ~~processes controlling the water vapour (H₂O) entering the stratosphereic. In the model,~~

448 The dehydration of air entering the stratosphere largely depends on the cold-point
449 temperature around the tropopause. ~~This , which~~ may not be represented accurately by
450 reanalyses due to ~~their~~ the relatively coarse vertical resolution ~~with less variability in~~
451 ~~cold-point tropopause temperatures.~~ To investigate ~~this~~ the impacts of ~~under-represented~~
452 ~~variability in cold-point temperatures~~ ~~this~~, we compare trajectory results from using
453 ~~standard~~ MERRA model level temperatures to those using temperature datasets in finer
454 vertical resolution ~~with enhanced variability~~. This includes GPS temperatures and ~~an~~
455 adjusted MERRA temperatures ~~dataset~~ ~~with enhanced vertical variability induced by that~~
456 ~~uses~~ wave scheme developed by Kim and Alexander (2013). ~~to reconstruct~~
457 ~~underrepresented vertical variability in MERRA temperatures.~~

458

459 Compared with ~~using the standard~~ MERRA ~~original~~ temperatures, we find that using
460 higher resolution GPS temperatures dries the H₂O prediction ~~stratosphere~~ by ~0.1 ppmv,
461 and using MERRA temperatures adjusted ~~with waves~~ by wave scheme dries the
462 stratosphere by ~0.2-0.3 ppmv (Fig. 7a-b). This is consistent with previous analyses (e.g.,
463 Jensen et al., 2004; Schoeberl et al., 2011). Despite the ~~small~~ differences in H₂O

464 abundances, the interannual variability (~~the~~ residual ~~after subtracting~~ from the mean
465 annual cycle) exhibits virtually no differences, due to the strong coupling between
466 stratospheric H₂O and tropical cold-point temperatures (Fig. 8). Therefore, in terms of
467 studying the interannual changes of stratospheric H₂O, we argue that reanalysis
468 temperatures are more useful due to its long-term availability.

469

470 Looking at the locations of FDP ~~points~~, we find a bimodal distribution when using
471 ~~standard~~ MERRA temperatures on model levels (Figs. 5-6). This is caused by the fact
472 that the cold-point ~~tropopause~~ is constrained to be near the two MERRA model levels
473 (100.5 and 85.4 hPa) that bracket the cold-point tropopause (Fig. 5d-f, black histograms).

474 When using the temperatures ~~fields with in~~ higher vertical resolution ~~with more~~
475 ~~variability~~, the resultant FDP patterns appear to be more physically reasonable (Figs. 5-6),

476

477 In this paper we perform linear interpolations for all trajectory runs. Other analyses have
478 used cubic spline interpolation owing to the strong curvature of temperature profile
479 around the cold-point tropopause. We investigate the performances of both schemes using
480 GPS temperature profiles (Sect. 2.2.3) and find that while introducing new information
481 due to its assumption in the temperature profile around the tropopause, cubic spline
482 scheme tends to generate unrealistically low cold-point temperature due to cubic fitting.
483 Therefore, the results are not necessarily realistic and on the other hand linear
484 interpolation is overall more accurate (Fig. 4).

485

486 It is well known that ~~TTL temperatures regulate stratospheric humidity. trajectory models~~

487 ~~can accurately simulate stratospheric humidity despite obvious arguments (e.g., vertical~~
488 ~~resolutions of temperatures, dehydration mechanisms, lack of convection,~~
489 ~~supersaturation, etc.)~~. In this paper, we have investigated one issue in our understanding
490 of TTL temperatures ~~of these~~ — the effect of finer vertical resolution that may have
491 captured more variability in tropopause temperatures — and find that it is comparatively
492 minor. This provides some confidence that the trajectory model driven by current modern
493 reanalyses ~~is good enough in depicting~~ is capable of depicting the stratospheric water
494 vapour accurately.
495

496 **Acknowledgements**

497 The authors thank Kenneth Bowman, Joan Alexander, and Eric Jensen for their helpful
498 discussions and comments. This work was supported by NSF AGS-1261948, NASA
499 grant NNX13AK25G and NNX14AF15G, and partially under the NASA Aura Science
500 Program. This work was partially carried out during visits of Tao Wang funded by the
501 Graduate Student Visitor Program under the Advanced Study Program (ASP) at the
502 National Center for Atmospheric Research (NCAR), which is operated by the University
503 Corporation for Atmospheric Research, under sponsorship of the National Science
504 Foundation.

505 **References**

506

- 507 Andrews, D. G., Holton, J. R., and Leovy, C. B.: Middle Atmosphere Dynamics,
508 Academic Press, Orlando, Florida, 489 pp, 1987.
- 509 Anthes, R. A., et al.: The COSMIC/FORMOSAT-3 mission: Early results, *Bull. Am.*
510 *Meteorol. Soc.*, 89, 313–333, doi:10.1175/BAMS-89-3-313, 2008.
- 511 Beyerle, G., Schmidt, T., Michalak, G., Heise, S., Wickert, J., and Reigber, Ch.: GPS
512 radio occultation with GRACE: Atmospheric profiling utilizing the zero difference
513 technique, *Geophys. Res. Lett.*, 32, L13806, doi:10.1029/2005GL023109, 2005.
- 514 Bowman, K. P.: Large-scale isentropic mixing properties of the Antarctic polar vortex
515 from analyzed winds, *J. Geophys. Res.*, 98, 23013–23027, 1993.
- 516 Bowman, K. P., Lin, J. C., Stohl, A., Draxler, R., Konopka, P., Andrews, A., and Brunner,
517 D.: Input data requirements Lagrangian Trajectory Models, *B. Am. Meteorol. Soc.*,
518 94, 1051–1058, doi:10.1175/BAMS-D-12-00076.1, 2013.
- 519 Brewer, A. W.: Evidence for a world circulation provided by the measurements of helium
520 and water vapor distribution in the stratosphere, *Q. J. R. Meteorol. Soc.*, 75, 351–
521 363, 1949.
- 522 Das, U. and Pan, C. J.: Validation of FORMOSAT-3/COSMIC level 2 "atmPrf" global
523 temperature data in the stratosphere, *Atmos. Meas. Tech.*, 7, 731-742,
524 doi:10.5194/amt-7-731-2014, 2014.
- 525 Dessler, A. E., Weinstock, E. M., Hints, E. J., Anderson, J. G., Webster, C. R., May, R.
526 D., Elkins, J. W., and Dutton, G. S.: An examination of the total hydrogen budget of
527 the lower stratosphere, *Geophys. Res. Lett.*, 21, 2563–2566, 1994.
- 528 Dessler, A. E., Schoeberl, M. R., Wang, T., Davis, S. M., and Rosenlof, K. H.:
529 Stratospheric water vapor feedback, *P. Natl. Acad. Sci. USA*, 110, 18087–18091,
530 doi:10.1073/pnas.1310344110, 2013.
- 531 [Dessler, A. E., Schoeberl, M. R., Wang, T., Davis, S. M., and Rosenlof, K. H., Vernier, J.-
532 P.: Variations of Stratospheric Water Vapor Over the Past Three Decades, *J. Geophys.
533 Res.* 119, DOI: 10.1002/2014JD021712, 2014.](#)
- 534 Fleming, E. L., Jackman, C. H., Weisenstein, D. K., and Ko, M. K. W.: The impact of
535 interannual variability on multidecadal total ozone simulations, *J. Geophys. Res.*,
536 112, D10310, doi:10.1029/2006JD007953, 2007.
- 537 Fueglistaler, S., Bonazzola, M., Haynes, P. H., and Peter, T.: Stratospheric water vapor
538 predicted from the Lagrangian temperature history of air entering the stratosphere in
539 the tropics, *J. Geophys. Res.*, 110, D08107, doi:10.1029/2004JD005516, 2005.
- 540 Fueglistaler, S., Dessler, A. E., Dunkerton, T. J., Folkins, I., Fu, Q., and Mote, P. W.: The
541 tropical tropopause layer, *Rev. Geophys.*, 47, RG1004, doi:10.1029/2008RG000267,
542 2009.
- 543 Gettelman, A. and Forster, P. M. de: Definition and climatology of the tropical tropopause
544 layer, *Journal of the Meteorological Society of Japan*, 80:4B, 911-924, 2002.
- 545 Gettelman, A., Randel, W. J., Wu, F., and Massie, S. T.: Transport of water vapor in the
546 tropical tropopause layer, *Geophys. Res. Lett.*, edited, p. 10.1029/2001GL013818,
547 2002.
- 548 Gettelman, A., and Wang, T.: Structural diagnostics of the tropopause inversion layer and
549 its evolution, *J. Geophys. Res. Atmos.*, 120, doi:10.1002/2014JD021846, 2015.
- 550 Hajj, G. A., Ao, C. O., Iijima, B. A., Kuang, D., Kursinski, E.R., Mannucci, A. J.,

551 Meehan, T. K., Romans, L. J., de La Torre Juarez, M., and Yunck, T. P.: CHAMP and
552 SAC-C atmospheric occultation results and intercomparisons, *J. Geophys. Res.*, 109,
553 D06109, doi:10.1029/2003JD003909, 2004.

554 Ho, S.-P., Goldberg, M., Kuo, Y.-H., Zou, C.-Z., and Schreiner, W.: Calibration of
555 temperature in the lower stratosphere from microwave measurements using
556 COSMIC radio occultation data: Preliminary results, *Terr. Atmos. Ocean. Sci.*, 20,
557 87–100, 2009.

558 Holton, J. R., Haynes, P. H., McIntyre, M. E., Douglass, A. R., Rood, R. B., Pfister, L.:
559 Stratosphere-troposphere exchange, *Rev. Geophys.*, 334, 405–439, 1995.

560 Holton, J. R., and Gettelman, A.: Horizontal transport and the dehydration of the
561 stratosphere, *Geophys. Res. Lett.*, 28(14), 2799–2802, doi:10.1029/2001GL013148,
562 2001.

563 Jensen, E., and Pfister, L.: Transport and freeze-drying in the tropical tropopause layer, *J.*
564 *Geophys. Res.*, 109, D02207, doi:10.1029/2003JD004022, 2004.

565 Kim, J.-E., and Alexander, J. M.: A new wave scheme for trajectory simulations of
566 stratospheric water vapor, *Geophys. Res. Lett.*, 40, 5286–5290,
567 doi:10.1002/grl.50963, 2013.

568 Kim, J.-E., and Alexander, J. M.: Direct impacts of waves on tropical cold point
569 tropopause temperature, *Geophys. Res. Lett.*, doi:10.1002/2014GL062737, 2015.

570 Kursinski, E. R., Hajj, G. A., Schofield, J. T., Linfield, R. P., and Hardy, K. R.: Observing
571 Earth's atmosphere with radio occultation measurements using the Global
572 Positioning System, *J. Geophys. Res.*, 102(D19), 23429–23465,
573 doi:10.1029/97JD01569, 1997.

574 Liu, Y. S., Fueglistaler, S., and Haynes, P. H.: Advection-condensation paradigm for
575 stratospheric water vapor, *J. Geophys. Res.*, 115, D24307,
576 doi:10.1029/2010jd014352, 2010.

577 Mote, P. W., Rosenlof, K. H., McIntyre, M. E., Carr, E. S., Gille, J. C., Holton, J. R.,
578 Kinnarsley, J. S., Pumphrey, H. C., Russell III, J. M., and Waters, J. W.: An
579 atmospheric tape recorder: the imprint of tropical tropopause temperatures on
580 stratospheric water vapor, *J. Geophys. Res.*, 101, 3989–4006, 1996.

581 Ploeger, F., Konopka, P., Günther, G., Groö, J.-U., and Müller, R.: Impact of the
582 vertical velocity scheme on modeling transport across the tropical tropopause layer,
583 *J. Geophys. Res.*, 115, doi:10.1029/2009JD012023, 2010.

584 Ploeger, F., Fueglistaler, S., Groö, J.-U., Günther, G., Konopka, P., Liu, Y. S., Müller,
585 R., Ravagnani, F., Schiller, C., Ulanovski, A., and Riese, M.: Insight from ozone and
586 water vapour on transport in the tropical tropopause layer (TTL), *Atmos. Chem.*
587 *Phys.*, 11, 407–419, doi: 10.5194/acp-11-407-2011, 2011.

588 Randel, W. J., Wu, F., Oltmans, S. J., Rosenlof, K. H., Nedoluha, G. E.: Interannual
589 Changes of Stratospheric Water Vapor and Correlations with Tropical Tropopause
590 Temperatures. *J. Atmos. Sci.*, 61, 2133–2148. doi: http://dx.doi.org/10.1175/1520-
591 0469(2004)061<2133:ICOSWV>2.0.CO;2, 2004.

592 Randel, W. J., Wu, F., Vömel, H., Nedoluha, G. E., and Forster, P.: Decreases in
593 stratospheric water vapor after 2001: Links to changes in the tropical tropopause and
594 the Brewer-Dobson circulation, *J. Geophys. Res.*, 111, D12312,
595 doi:10.1029/2005JD006744, 2006.

596 Randel, W. J. and Jensen, E. J.: Physical processes in the tropical tropopause layer and

597 their role in a changing climate, *Nat. Geosci.*, 6, 169–176, doi:10.1038/ngeo1733,
598 2013.

599 Ray, E.A., Moore, F.L., Rosenlof, K.H., Davis, S.M., Sweeney, C., Tans, P., Wang, T.,
600 Elkins, J.W., Bönisch, H., Engel, A., Sugawara, S., T. Nakazawa and S. Aoki:
601 Improving stratospheric transport trend analysis based on SF6 and CO2
602 measurements, *J. Geophys. Res.* doi: 10.1002/2014JD021802, 2014.

603 Read, W. G., et al.: Aura Microwave Limb Sounder upper tropospheric and lower
604 stratospheric H2O and relative humidity with respect to ice validation, *J. Geophys.*
605 *Res.*, 112, D24S35, doi:10.1029/2007JD008752, 2007.

606 Rienecker, M. M., Suarez, M. J., Gelaro, R., Todling, R., Bacmeister, J., Liu, E.,
607 Bosilovich, M. G., Schubert, S.D., Takacs, L., Kim, G.-K., Bloom, S., Chen, J.,
608 Collins, D., Conaty, A., da Silva, A., Gu, W., Joiner, J., Koster, R. D., Lucchesi, R.,
609 Molod, A., Owens, T., Pawson, S., Pegion, P., Redder, C. R., Reichle, R., Robertson,
610 F. R., Ruddick, A. G., Sienkiewicz, M., and Woollen, J.: MERRA – NASA’s modern-
611 era retrospective analysis for research and applications, *J. Climate*, 24, 3624–3648,
612 doi:10.1175/JCLI-D-11-00015.1, 2011.

613 Schoeberl, M. R., Douglass, A. R., Zhu, Z. X., and Pawson, S.: A comparison of the
614 lower stratospheric age spectra derived from a general circulation model and two
615 data assimilation systems, *J. Geophys. Res.*, 108, 4113, 2003.

616 Schoeberl, M. R. and Dessler, A. E.: Dehydration of the stratosphere, *Atmos. Chem.*
617 *Phys.*, 11, 8433–8446, doi:10.5194/acp-11-8433-2011, 2011.

618 Schoeberl, M. R., Dessler, A. E., and Wang, T.: Simulation of stratospheric water vapor
619 and trends using three reanalyses, *Atmos. Chem. Phys.*, 12, 6475–6487,
620 doi:10.5194/acp-12- 6475-2012, 2012.

621 Schoeberl, M. R., Dessler, A. E., and Wang, T.: Modeling upper tropospheric and lower
622 stratospheric water vapor anomalies, *Atmos. Chem. Phys.*, 13, 7783–7793,
623 doi:10.5194/acp-13- 7783-2013, 2013.

624 Schoeberl, M. R., Dessler, A. E., Wang, T., Avery, M. A, Jensen, E.: Cloud Formation,
625 Convection, and Stratospheric Dehydration, *Earth and Space Science*, DOI:
626 10.1002/2014EA000014, 2014.

627 Solomon, S., Rosenlof, K. H., Portmann, R. W., Daniel, J. S., Davis, S. M., Sanford, T. J.,
628 and Plattner, G.-K.: Contributions of stratospheric water vapor to decadal changes in
629 the rate of global warming, *Science*, 327, 1219–1223, 2010.

630 Wang, T., Randel, W. J., Dessler, A. E., Schoeberl, M. R., and Kinnison, D. E.: Trajectory
631 model simulations of ozone (O₃) and carbon monoxide (CO) in the lower
632 stratosphere, *Atmos. Chem. Phys.*, 14, 7135-7147, doi:10.5194/acp-14-7135-2014,
633 2014.

634 Wickert, J., Reigber, C., Beyerle, G., König, R., Marquardt, C., Schmidt, T., Grundwaldt,
635 L., Galas, R., Meehan, T. K., Melbourne, W. G., and Hocke, K.: Atmosphere
636 sounding by GPS radio occultation: First results from CHAMP: *Geophys. Res.*
637 *Let.*, 28, 3263–3266, 2011.

638
639
640

Table

Table 1. Different temperature datasets used in trajectory model.

Temperature Datasets	Availability	Horizontal Resolution (Longitude x Latitude)	Vertical Resolution In TTL	Trajectory Runs Denoted
MERRA	Daily*	2/3 x 1/2	~1.2 km	<i>traj.MER-T</i>
GPS (gridded)	Daily	2.5 x 1.25	0.2 km	<i>traj.GPS-T</i>
MERRA w/ waves	Daily*	2/3 x 1/2	0.2 km	<i>traj.MER-Twave</i>

641
642

*These datasets are available 6-hourly. But for fair comparison with using GPS data, we used daily averages.

643 **Figures**
644
645

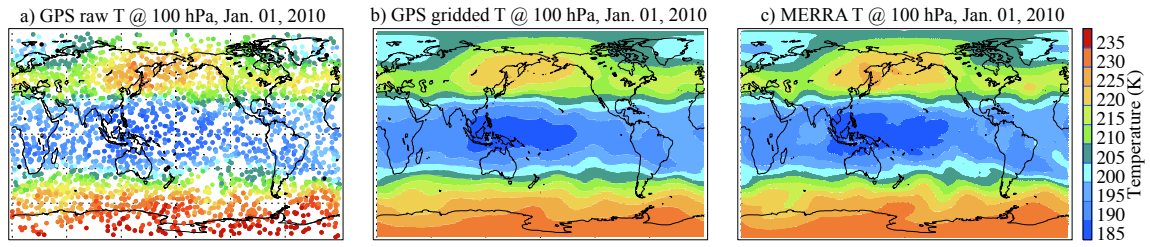


Fig. 1. (a) Comparison of temperatures from raw GPS (panel a), gridded GPS (panel b), and MERRA temperature (panel c) at 100 hPa on Jan. 1st, 2010.

646

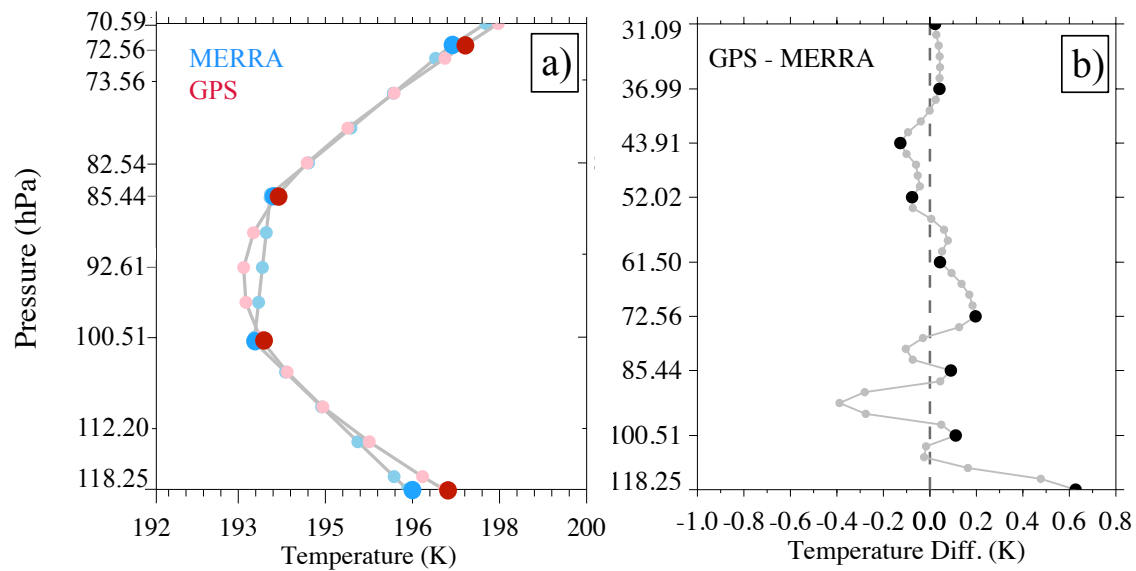


Fig. 2. (a) MERRA (blue) and GPS (red) mean temperature in TTL and (b) their differences (GPS – MERRA) extended to 31 hPa. All values are averaged over the deep tropics (18°S – 18°N) in 2007-2013, with larger dots marking the MERRA model levels and small dots marking the MERRA in-between levels, where both GPS and MERRA temperatures are linearly interpolated to the same pressure levels. ~~Temperature differences between GPS and MERRA at MERRA model levels (black dots) and MERRA in-between levels, averaged over the deep tropics (18°S – 18°N) in 2007-2013. Temperature in-between MERRA levels are obtained from linear interpolation.~~

647
648

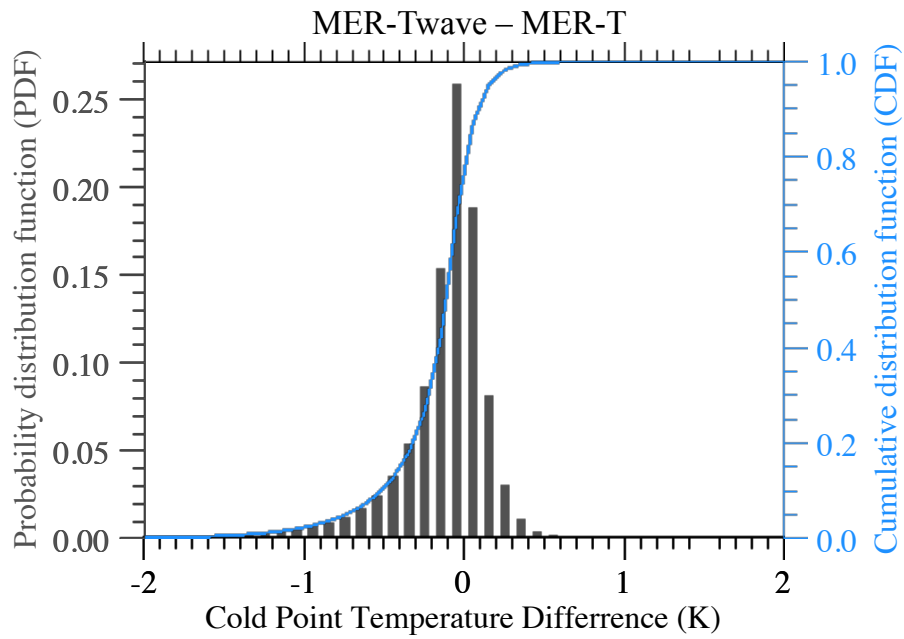


Fig. 3. Cold-Point temperature differences between MERRA adjusted by waves and MERRA (MER-Twave – MER-T) during 2007-2013. The PDF in black is plotted on left-y axis and CDF in blue on right-y axis.

651

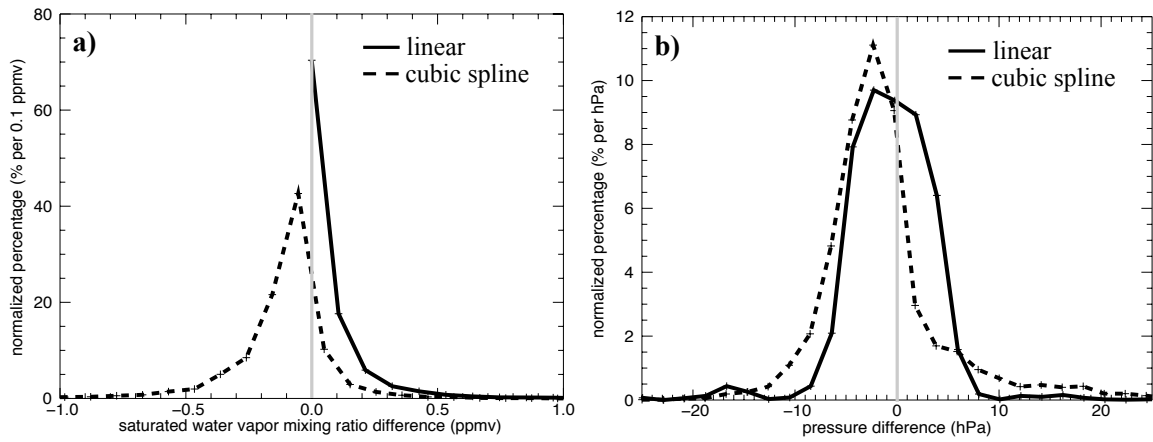


Fig. 4. PDFs of the differences between linear or cubic spline interpolations to the actual value from the GPS temperature profiles. (a) Minimum saturation mixing ratio of the profile (units are percent per 0.1 ppmv); (b) pressure of the saturation mixing ratio minimum (units are percent per hPa). The plus signs in each line mark the bin intervals.

652

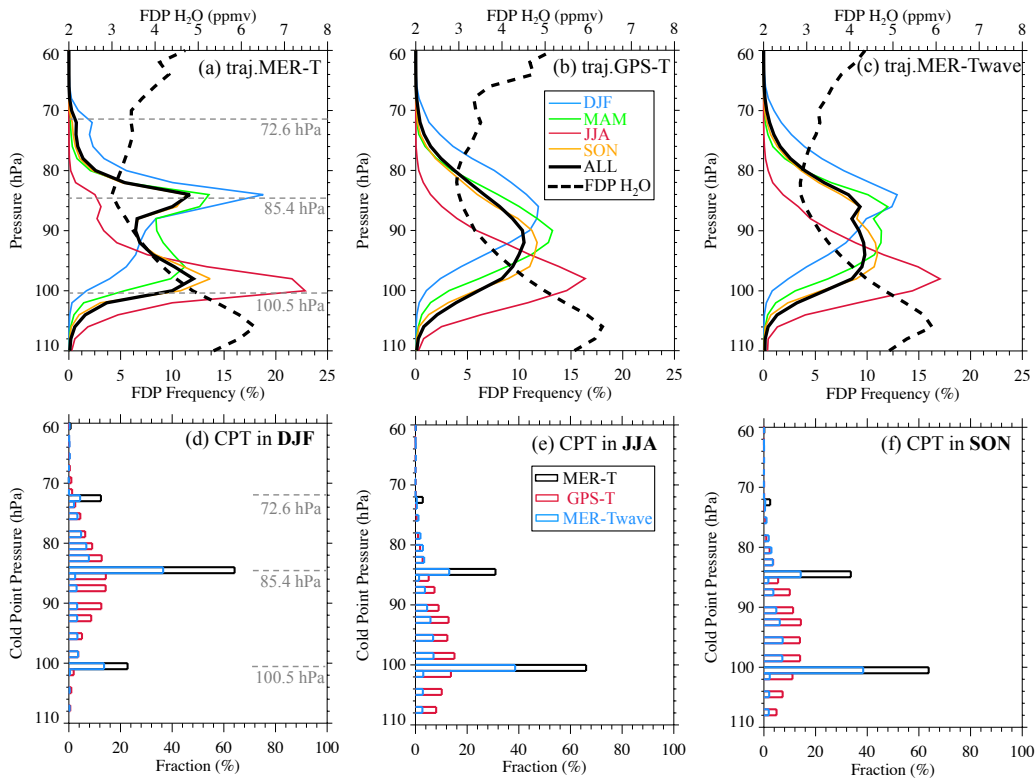


Fig. 5. Seasonal FDP vertical distributions (in %/hPa, solid lines, lower x axis) and FDP saturation mixing ratio (FDP-H₂O, i.e., the stratosphere entry level H₂O, ppmv, dashed lines, upper x axis) from trajectory simulations using (a) MERRA temperatures, (b) GPS temperatures, and MERRA temperatures adjusted by waves (c), compared to the cold point tropopause statistics during (d) DJF, (e) JJA, and (f) SON. The FDP frequency is normalized by total FDP events, so each solid curve adds up to 100%. The MERRA model levels are marked in panels a and d.

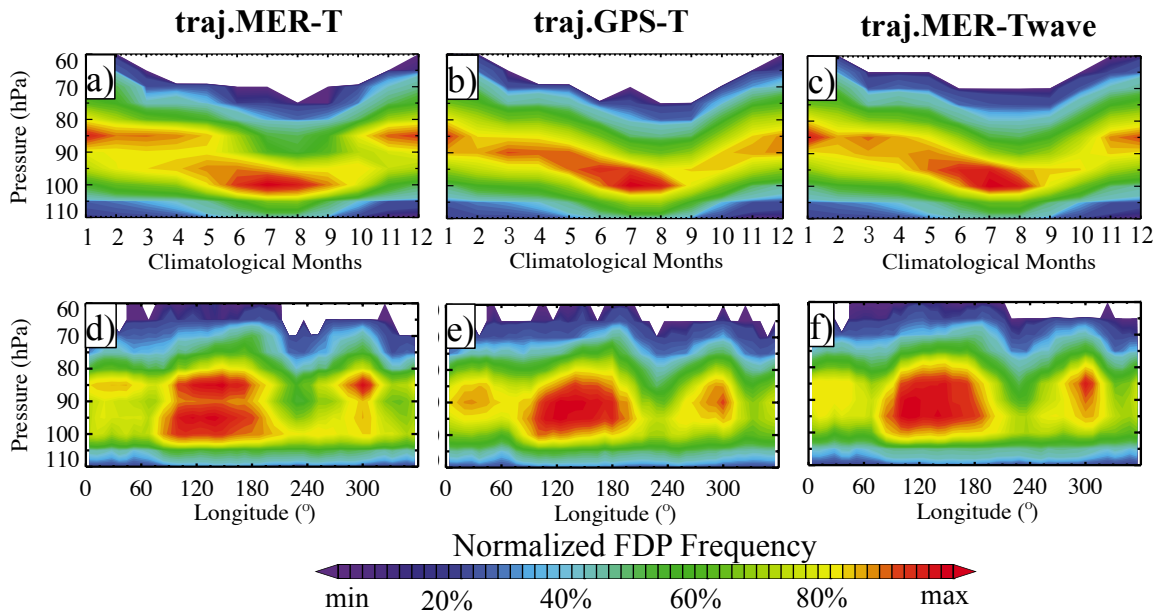


Fig. 6. Vertical distributions of normalized FDP events in time-evolutional (a-c) views among trajectory simulations by using a) MERRA temperature (*traj.MER-T*), b) GPS RO temperature (*traj.GPS-T*), and c) MERRA temperature adjusted by waves (*traj.MER-Twave*). The longitudinal variations of FDP during SON are highlighted in panel d-f to emphasize the FDP discontinuity in *traj.MER-T*. All panels are plotted in their own range and color-coded at the same percentiles (i.e., 0, 20%, 40%, ..., 100%) to compare the patterns.

654

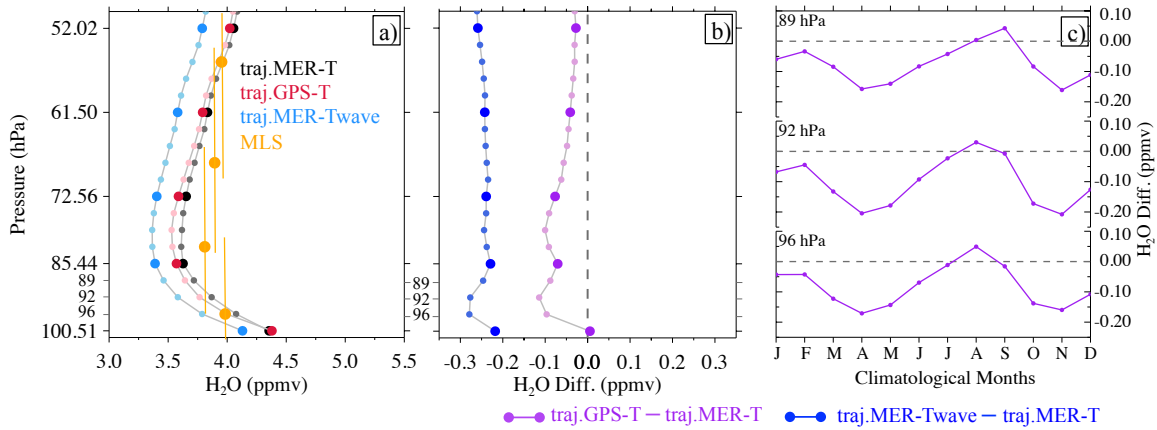


Fig. 7. (a) Trajectory predicted H₂O compared with MLS observations (the vertical bars in orange indicate the MLS vertical resolutions at each of the MLS retrieval pressure levels); (b) trajectory H₂O differences induced by waves (blue) and by using GPS temperatures (purple); (c) annual differences at 96, 92, and 89 hPa. All values are averaged over the deep tropics (18°S–18°N) in 2007-2013, with larger dots marking the MERRA model levels and small dots marking the MERRA in-between levels – those are the levels that the cold-point tropopause could have been found but not available in current MERRA vertical resolution.

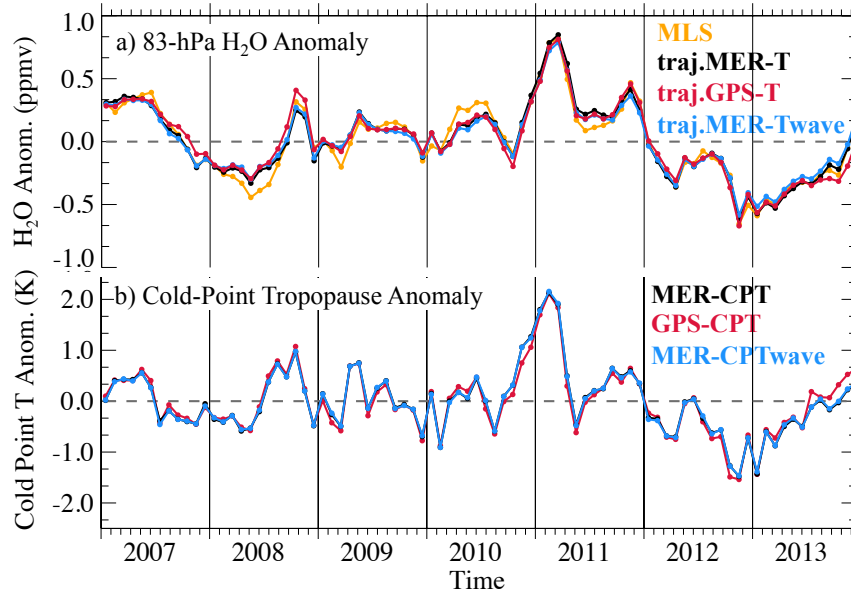


Fig. 8. (a) Trajectory simulated H₂O anomalies compared with the MLS observations; and (b) cold-point temperature anomalies from three temperature datasets. All time series are averaged over the deep tropics (18°N-18°S). All trajectory results in panel a are weighted by the MLS averaging kernels for fair comparison.

657
658